Clinical Cancer Investigation Journal-ISSN: 2278-0513

Molecular Dynamics Study and on the Design of Graphene-Tio$_2$ Nanotube Membranes for Water Desalination

Abstract

Understanding the atomic behavior of water on grapheme-titanium dioxide nanotubes (G-TiO_2NT) is crucial for future graphene/TiO_2NT water desalination applications. We use the molecular dynamics approach to mimic the physical behavior of liquid crystals with accurate atomic organization utilizing Tersoff and LJ force fields in this paper. Using molecular dynamics modeling, we studied the influence of TiO_2NT and G on the performance of the membrane in this study. To characterize their interactions, each liquid molecule is represented by an SPCE medel in this manner. We investigate the physical characteristics of water on TiO_2NT with a diameter of 14 using molecular dynamics simulations. The time it took for the desired system to attain equilibrium was calculated using factors like kinetic and potential energy. We demonstrate that a graphene-TiO_2 nanotube (G-TiO_2NT) membrane may operate as a nano filter to remove Na^+ and Cl^- ions from NaCl solutions with a 98 percent efficiency. The intensities of the peak of the O-O and H-H has a similar radial distribution function (RDF). Finally, our findings suggest that the graphene-TiO_2NT membrane can perform well in real-world situations.

Keywords: *TiO_2, Nanotube, Simulation, Graphene, Desalination, Molecular dynamics.*

Roya.Bakhshkandi[1], Mansour.Rezaei Mersagh[2], Mohammad.Samipoor Giri[3*], Mostafa.Sefidgar[4]

[1]Physics Department, Islamic Azad University, North Tehran Branch, Tehran, Iran, Email: rbakhshkandi@gmail.com

[2]Physics Department, Islamic Azad University, North Tehran Branch, Tehran, Iran, Email: m_rezaye_mersagh@iau-tnb.ac.ir

[3]Chemical Engineering Department, Islamic Azad University, North Tehran Branch, Tehran, Iran, Email: M_samipoor@iau-tnb.ac.ir

[4]Mechanical Engineering Department, Islamic Azad University, Pardis Branch, Tehran, Iran, Email: msefidgar@pardisi.au.ac.ir

***Corresponding author:** Mohammad.Samipoorgiri, Email: M_samipoor@iau-tnb.ac.ir, Phone number: +989121072396.*

1. Introduction

In the context of a rapidly rising worldwide water shortage, water desalination is a procedure for purifying water by removing mineral components and ions from saline water to deliver new fresh water. Many publications concerning the manufacturing and modification of atomic membranes have been published in recent years, to develop an efficient filtering technology for the separation of ions, organic, and inorganic compounds from water [1]. The graphene membrane has been employed in numerous research due to its great chemical and mechanical stability, and it verifies good salt rejection for widely used ions by employing single-layer nonporous graphene [2]. Recent theoretical and experimental investigations [3–5] have focused on designing and altering carbon-based thin-film membranes that can be used in reverse osmosis pressure-driven processes. By modifying the topology of the hydrogen bond network, the strong confinement of water molecules in structures like carbon nanotubes significantly alters the structural, thermodynamic, and dynamic characteristics. Chakraborty et al. [6] gave a computational analysis of the behavior of confined water within CNTs and between graphene and graphene oxide (GO) sheets in this respect. Because of their collective motion, water molecules contained in short and thin CNTs with open ends display Fickian diffusion, according to their findings. They discovered that in the presence of water, the potential of mean force for the oxidized section of graphene oxide sheets has two local minima, corresponding to a dry cavity and a completely hydrated cavity. Using molecular dynamics (MD) simulations, A.K.Giri et al. studied the effects of oxidation degree and interlayer spacing on filtering efficiency and water structure in graphene oxide. They discovered that increasing interlayer separation (the optimum value was 0.8 nm) enhanced water permeability, whereas increasing oxidation degree (the best value was 10% or below) lowered it [7]. They investigated the effect of the structure and dynamics of confined water on the diameter and length of the capped carbon nano-tubes in another computational investigation based on the molecular dynamics simulation approach [8]. Water permeability fluctuation was assessed experimentally by taking into account the impacts of graphene sheet alignment and membrane hydrophobicity [9, 10]. Graphene membranes for water desalination have a few drawbacks, despite their high rate of ion rejection and high water permeability. To begin with, ions with similar sizes to sodium and chloride ions (e.g. calcium, fluoride, and iron) may be removed during the salt removal process. It's important to note that these substances are necessary for human health [11]. Second, fabricating large-area graphene membranes is a somewhat costly technique [12]. Finally, desalination facilities

have a broad range of detrimental effects on the surrounding eco-system and ecosystem [13,14].

he majority of the saltwater outflow, for example, is re-distributed into the maritime environment without being treated. This has the potential to create significant environmental damage, not only in the long run but also in the short term [15,16].On the other hand, titanium dioxide has interested researchers because of its high atomic performance, as well as the cost-effective and ecologically friendly production of TiO_2 [17]. Furthermore, rutile and anatase with a tetragonal structure, and brookite with an orthorhombic structure, are three crystalline forms of titanium dioxide [18]. The exceptional UV irradiation capability of anatase crystalline has made it the best phase of titanium dioxide for space operations [19]. Furthermore, owing to its stability, high hydrophilicity, antibacterial property, photocatalytic activity, low toxicity, and cheap cost, Dioxide Titanium has been extensively researched for membrane modification [20–22]. Modification of porosity, pore size, and physical and chemical characteristics, for example, may lead to increased thermal and mechanical stability, eventually boosting membrane performance [23]. The activity of the titanium dioxide/graphene combination has been described as an antifouling agent that prevents organic pollutant deposition on their surface [24]. In 2020, Q, Ibrahim, and their colleagues developed a graphene/TiO_2 bilayer nanocomposite membrane structure that was simulated to improve the graphene membrane's physical characteristics. Material Studio 2019 software was used to simulate the electrical and mechanical characteristics. Under varied applied pressures, the findings revealed an increase in salt rejection and water permeability when compared to a graphene membrane [25]. We used MD simulations for seawater desalination in our research. We optimize the graphene/TiO_2 membrane performance for salt rejection for the first time. To demonstrate TiO_2/atomic graphene's promise, we employ one form of TiO_2NT in an atomic membrane structure. We give physical parameters salt to define the suitable performance of our simulated membrane. Salt rejection and permeance across titanium nanotube/graphene membranes promote atomically ultimately, these results with other membranes.

2. Computational method

These simulations were carried out using the most recent version of Sandia National Laboratories' Large-scale Atomic/Molecular Massively Parallel Simulator (LAMMPS) program [26,27]. Various force fields, such as Lennard Jones, EAM, Tersoff, Gay-Berne, and others, are included in this MD simulation program. The simulation force field you choose has a big impact on the outcomes you get from MD simulations. We should select the simulation force field depending on the physical parameters under investigation to acquire accurate findings. Fereidoon and colleagues [28] studied the elastic characteristics of graphene, titanium dioxide (rutile), and graphene/ titanium dioxide nanocomposite, and found that the Universal force field outperformed COMPASS. According to the findings, the Universal force field is more suited and trustworthy than COMPASS for calculating Young's modulus. The interaction with the graphene layer resulted in a 14 percent increase in dioxide titanium rutile and a 12 percent increment in shear modulus. As a result, the interatomic potential for particles in our atomic simulations of metal and fluid structures was based on an embedded-atom method (EAM) and universal force field (UFF) [29,30].In our MD simulations, graphene sheets were organized at up and down areas of the simulation box of 50Å×50Å×50Å volume, and dioxide titanium nanotube atoms were positioned in the central position of the simulation box. Our simulation boxes are shown in top, front, and perspective perspectives in Fig.2(a,b,c). Fixed boundary conditions in the x, y, and z axes are also included in the simulation box. This computational code is divided into six sections:

• Obtaining the simulation system
• Defining atoms or atomic modeling, as shown in Figure 1.
• Definitions of potential and atom interactions
• Definitions of molecular dynamic simulation modifications
• Adjustment of public water purification outputs

The quantity of flux, the amount of average force applied to the fluid, the value of the radial distribution function, and the implementation of molecular dynamics simulation are among the dedicated outputs that may be adjusted. The simulation preparation process is completed first, followed by the selection of the physical parameter unit in the computational code. We implanted the starting circumstances of the atomic structures after identifying the physical units utilized in the simulation, which included determining the size of the space and the required boundary conditions. A three-dimensional model and atomic structure are used to describe the attributes of atoms and molecules provided in the simulation, such as atomic number, atomic position, bonds, and so on, in such a manner that each of the mentioned scenarios is picked regularly. The location of the atoms and molecules in the simulation is defined in the second stage of the MD simulation. This section covers topics like setting the size of the simulation region and how the atoms are grouped. The bonds between atoms, for example, are shown and remembered.

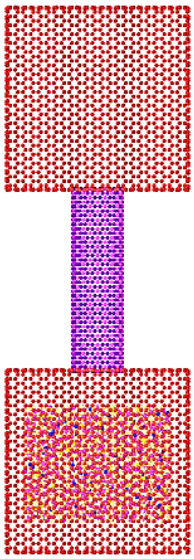

Figure 1. Schematic of TiO_2NT/Graphene membrane in our MD simulations from perspective view

We describe the potential of the forces applied between the atoms in the third stage of MD simulations, and we calculate the interactions between the individual atoms depicted in the simulation box. As can be observed, Lennard-Jons and Tersoff force fields were employed in this simulation, and they will be given in the formulation of this force field. The constant coefficients of this potential are then specified, and a list of interacting atoms (so-called neighbors) is generated with a cutting radius of 12 Å in accordance with the cutting radius order. The force field employed in this study for the Lennard-Jons interaction has the following broad structure: Equation(1) [29] gives the LJ interatomic force field of i and j atoms:

$$V_{ij} = 4\varepsilon\left[\left(\frac{\sigma}{r_{ij}}\right)^{12} - \left(\frac{\sigma}{r_{ij}}\right)^{6}\right] \qquad r \ll r_c \quad (1)$$

where ε is the depth of the potential, and σ is the distance at which the potential reaches zero. The ployed parameters of LJ potential for every interaction kind are listed in Table 1.

Table 1. Lennard–Jones parameters applied in the simulations[30]

parameter	$\varepsilon(^{kcal}/_{mol})$	σ(Å)
Cl-Cl	0.227	3.947
H-H	0.044	2.886
Na-Na	0.030	2.983
O-O	0.060	3.5
Ti-Ti	0.017	3.175
C-Cl	0.154	3.904
C-H	0.068	3.334
C-Na	0.056	3.389
C-O	0.079	3.671
C-Ti	0.042	3.497
Cl-H	0.100	3.375
Cl-Na	0.129	3.431
Cl-O	0.117	3.717
Cl-Ti	0.004	3.540
H-Na	0.036	2.934
H-O	0.051	3.178
H-Ti	0.027	3.027
Na-O	0.042	3.231
Na-Ti	0.022	3.078
O-Ti	0.032	3.334

In terms of equations 2 and 3, respectively, the bond and angle strength in dreading potential is defined by simple harmonic oscillator equations:

$$E = \frac{1}{2}K_r(r - r_0)^2 \qquad (2)$$

$$E = \frac{1}{2}K_\theta(\theta - \theta_0)^2 \qquad (3)$$

In these equations, K_r, and K_θ are harmonic oscillator constants and r_0 and θ_0 are the atomic bond length and equilibrium value of the angle, respectively.

Table 2. The equilibration distance for bond strength and bond bend in MD simulations

band	r_0(Å)
C-C	1.53
Cl-Cl	1.32
Cl-O	0.98
H-O	0.98

Table 3. The equilibration angle for bond strength and angle bend in MD simulations[31,32]

angle	θ_0(degree)
C-C-C	109.471
Cl-O-H	109.471
H-O-H	104.510
O-Cl-O	104.510

The interatomic force among carbon atoms in the graphene sheet is accounted for by TERSOFF potential using the following equations [33]:

$$E = \frac{1}{2}\sum_i \sum_{j \neq i} V_{ij} \qquad (4)$$

$$V_{ij} = f_c(r_{ij})\left[f_R(r_{ij}) + b_{ij}f_A(r_{ij})\right] \qquad (5)$$

where the potential energy is decomposed into a site energy E_{ij} and a bonding energy V_{ij}, r_{ij} is the distance between i and j atoms, f_A and f_R are the attractive and repulsive pair potential, respectively, and f_C is a smooth cutoff function. In this equation, the b_{ij} is constant and depends on the kind of atoms in the simulation.

The temporal evolution of the atoms in the MD simulation box is determined in the fourth stage. In this case, we transform the NVT ensemble to the NVE ensemble and apply external force to the simulated systems with 0/02ev⁄Å. We input how to define the neighbors in the calculations after this phase. The thermodynamic outputs of our MD simulations are determined as follows:

The amount of salt is removed

The amount of water passing

In this research, the non-equivalent MD simulation was implemented for 1ns.

The system's atomic structure is separated into three portions (Fig.2). The first is a saltwater reservoir, box (I), which is made out of a graphene sheet that functions as a piston, forcing the solution through the graphene membrane. A membrane made of TiO_2 nanotubes with a pore radius of 7 Å is used in the second segment. A graphene sheet serves as a reservoir for purified water in the third segment (seen Fig.2). The water purification process in all simulations consists of 50 Na+ ions, 50 Cl– ions, and about 2,999 water molecules that are put in the simulation box.

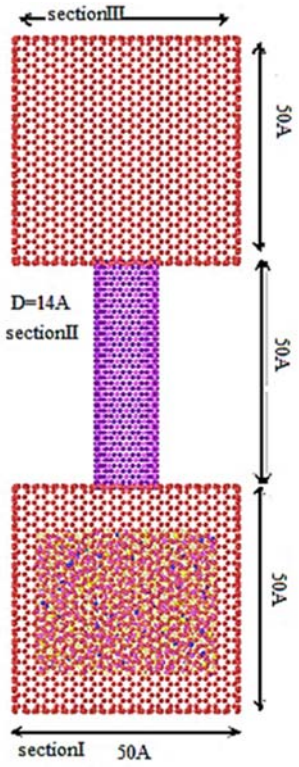

Figure 2. Schematic of TiO_2NT/Graphene membrane in our MD simulations from a perspective view.

3. Simulation results

To examine water purification quantitatively in an atomic membrane made of graphene nanosheets TiO_2NT, we divided the simulation box into 101 final section bins in the fluid movement direction, with the first half referring to the third section and the second half referring to the first section. In Fig 3, blue circles represent water molecules.

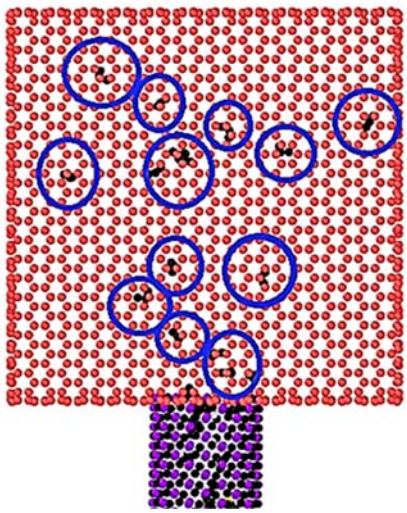

Figure 3. Schematic of simulated Graphene/TiO_2 nanotube, H_2O molecules, and iron matrix with LAMMPS package at top faces.

It is feasible to assure the optimum and proper performance of the atomic membrane to separate the ion atoms from the H_2O molecules in the simulated sections illustrated in Fig.3. Water molecules build in the second simulation box as MD simulation time passes in these Figs, as can be observed qualitatively. Because the atomic ions are kept in section I by this atomic technique, the purification of the H_2O molecules is excellent. According to the initial and final density curves for water and ion molecules, it is clear that water molecules are moved from section I to the nanotube and section III, whereas ions remain constant in section I of this structure's atomic density. Numerically, the highest rate of H_2O molecules occurs in 45 bins in the initial step of MD simulations, but as time passes, this maximum rate shifts to 55 bins. This atomic

behavior does not occur in ion atoms (Fig.4a,b). At the first and first-time steps, reception, this atomic maximum density is evident in 46 and 49 bins. As a result, we deduce that atoms (ions) displace in the G/ TiO_2NT membrane. (Fig.5a,b).

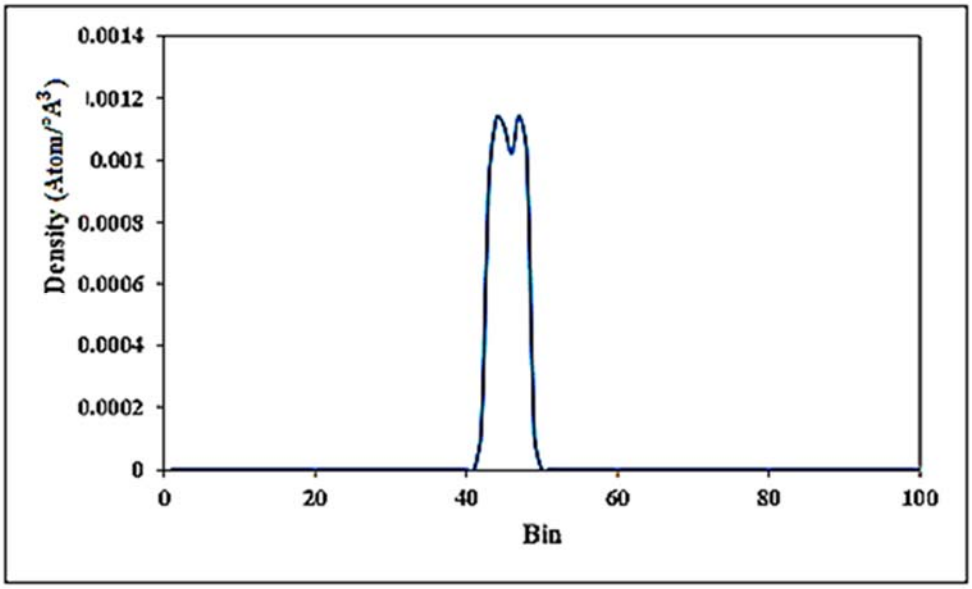

a

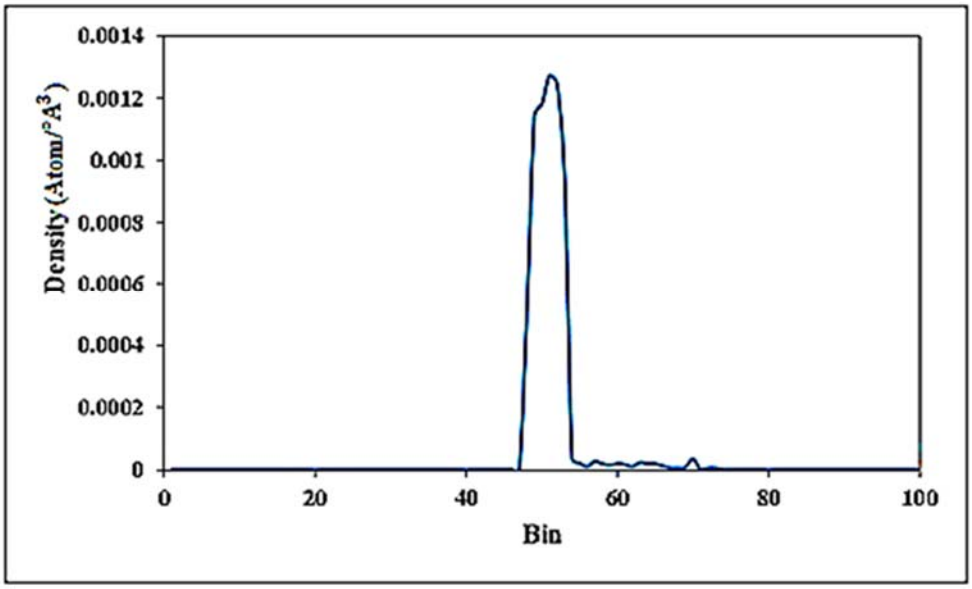

b

Figure4. The density of water molecules at the a)beginning b)end of the simulation

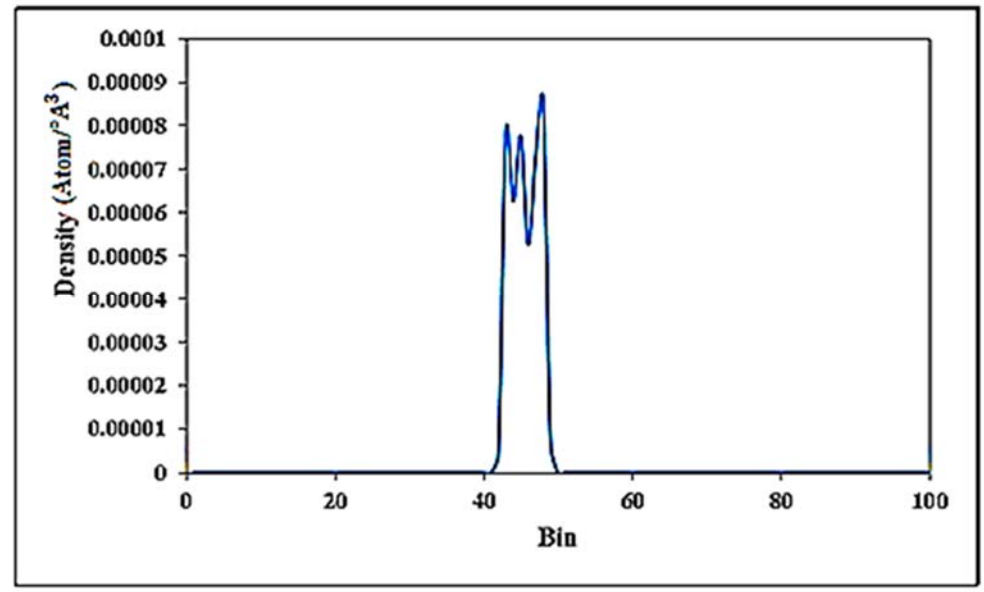

a

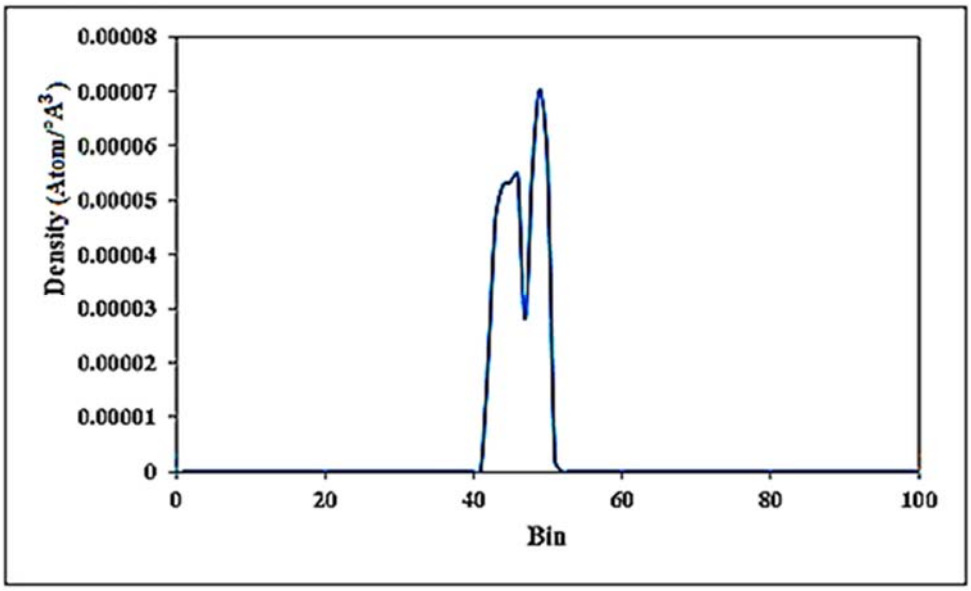

b

Figure 5. The density of ionic atoms at the a) beginning b)end of the simulation

Study of a radial distribution function

The structure of a molecular system with a change in particle number density with distance from a center particle is described by a radial distribution function (RDF). The method for calculating an RDF is shown in Equation (7).

$$g_{\alpha\beta}(r) = \lim_{dr\to 0}\left(\frac{\rho(r,dr)}{4\pi(N_{\alpha\beta}/V)r^2dr}\right) \qquad (7)$$

The number of atom pairs in the infinitesimal shell spanning r to r + dr (averaged across all trajectory frames) is ρ (r, dr), Nαβ is the number of pairings for the two species examined, and V is the volume of the system. Because (r, dr) is normalized to the uniform density of an ideal gas, any variation in g_αβ (r) from unity is due to some order or correlation in the material. While an RDF cannot be used to create a unique fingerprint for a substance, it may be used to provide a detailed description. RDFs may be used to determine numerous thermodynamic parameters, such as bond lengths and coordination numbers, providing that the potentials representing the system are pairwise additive. RDFs may also be produced from experimental X-ray or neutron diffraction data to offer strong simulation-experiment comparisons [34]. The radial distribution function is an intermediate between solid and gas, with one strong peak and a small number of peaks at short

distances that gradually diminish to a constant value at further distances. At lesser distances, the radial distribution function has little utility. The chance of two molecules aligning to reach this distance is lower than in the ideal gas state, and g(r) decreases as distance increases, indicating the lack of long-range forces at these distances. The neighbors surrounding each atom or molecule will be recorded within histograms to compute the radial function of a simulation. The total number of neighbors in each group will then be averaged across the whole simulation. The interaction of functional groups with water has been studied using RDF. It is also shown how functional groups affect the structural system of water molecules in the membrane. In the feed and RDF sections, Figs. 6a, b, and c investigate the membrane diagram between the atoms of oxygen-hydrogen, hydrogen-hydrogen, and oxygen-oxygen in water molecules. Numerically, The first, second, and third peaks for oxygen and hydrogen in water molecules in the membrane are 3.96Å, 4.2 Å, and 4.92 Å, respectively (Fig.6a). The migration of the H_2O molecule across the G/TiO_2NT membrane is shown in this atomic manner. Graph 9b Functional groups' effects on hydrogen and hydrogen atoms in water molecules have been studied. The g(r) value is about 7.017, while the peak is about 3.96. The first peak in Fig.6c is for oxygen-oxygen at 3.96 Å. Because the hydrogen-hydrogen and oxygen-oxygen peaks are in the same location, it's safe to assume that the hydrogen and oxygen atoms work together to establish this arrangement.

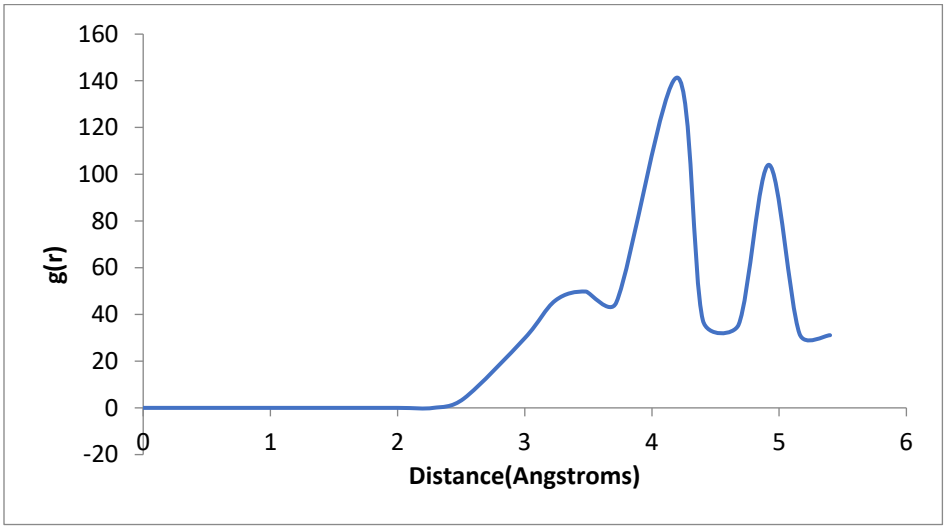

a

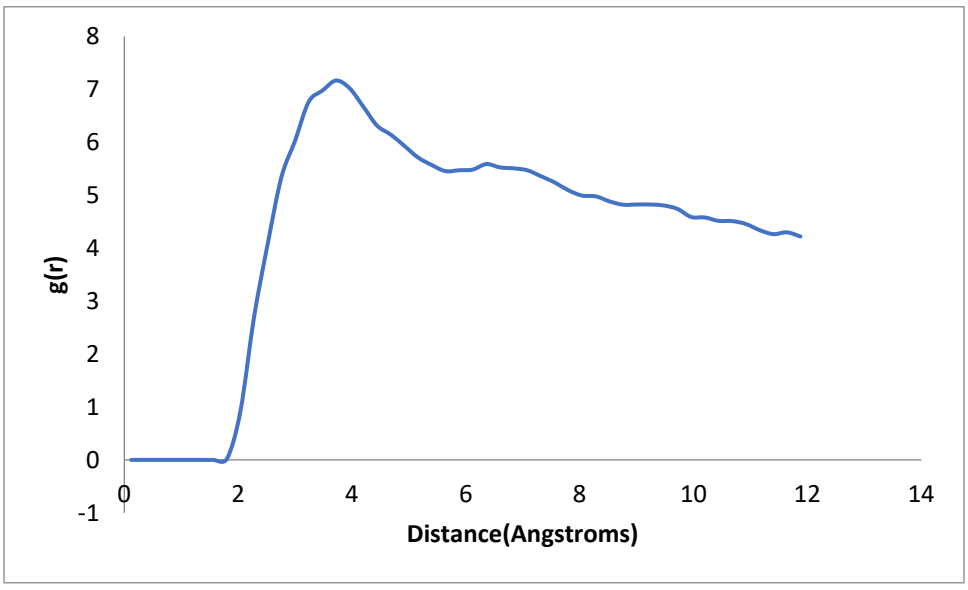

b

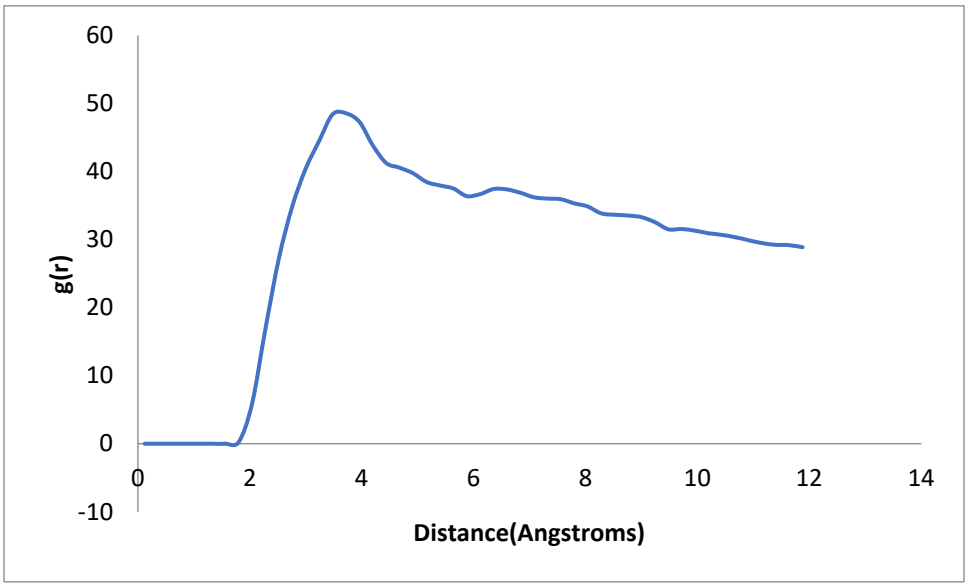

c

Figure 6. Graph of the radial distribution function for a)O-H b)H-H c)O-O graph

4. Conclusion

Molecular dynamics analysis of the performance of G/TiO_2NT nano-membranes for water desalination suggests that this atomic structure is a suitable arrangement for this purpose. Using LAMMPS software, the atomic structure was employed to distinguish salt from water in this study. The quantity of salt removal is studied in addition to the kind, structure, and material of the membrane, and the findings of this simulation are as follows. The presence of a substantial amount of water near an anatase (101) nanotube with a diameter of ~14Å is investigated. Titanium dioxide nanotubes and graphene sheets were utilized to explore the separation of salt and chloride ions from water, and the findings suggested that these nanotubes and plates might be used to separate sodium and chloride ions. The size of sodium ions is smaller, which has a significant impact on their transit. Furthermore, as compared to oxygen ions, hydrogen atoms in functional groups, which are responsible for repelling sodium ions, are both smaller in size and have a lower burden. One of the reasons for the flow of water molecules amid graphene sheets, according to prior studies, is their regular structure. However, after looking at the water molecules between the graphene sheets, it was discovered that the water molecules' order had been gone, and the local order had taken its place. The RDF findings also show that hydroxyl groups are the primary source of water molecule order disruption between sheets. The combination graphene sheets-titanium dioxide nanotube system has a high capacity for the desalination of water.

Clean water is an essential substance for health and also an essential substance to prevent cancer. Excessive salt intake by the body can cause diseases such as gastric cancer, blood pressure, myocardial infarction, osteoporosis, asthma, and kidney disease. Consuming as much salt in the body ensures health and improves nerve function and muscles regulate blood pressure, fluid balance, and body electrolytes.

The authors declare that they have no conflict of interest.

Acknowledgments: None
Conflict of interest: None
Financial support: None
Ethics statement: None

References

1. Madhura L, Kanchi S, Sabela MI, Singh S, Bisetty K.,(2017) Membrane technology for water purification. Environ Chem Lett.https://doi.org/10.1007/s10311-017-0699-y.
2. Yoshinaga T, Lennon Luo S.X, Ngo Q. P, Yuan W,Swager T.M.(2022), Covalently Functionalized Graphene for Black Liquor Concentration Membranes. ACS Applied Nano Materials, 5 (10) , 15728-15737. https://doi.org/10.1021/acsanm.2c03786
3. Wu K, Chen Z, Li J, Li X, Xu J, Dong X .,(2017) Wettability effect on nanoconfined water flow. PNAS 114:3358–3363. https://doi.org/10.1016/j.nantod.2017.05.001.
4. Lohrasebi A, Rikhtehgaran S.,(2018) Ion separation and water purification by applying external electric field on porous graphene membrane. Nano Res. 11(4):2229–2236. https://doi.org/10.1007/s12274-017-1842-6.
5. Neek-Amal M, Lohrasebi A, Mousaei M, Radha B, Peeters FM.,(2018) Fast water flow through graphene nano capillaries: a continuum model approach involving the microscopic structure of confined water. Appl. Phys. Lett. 113(8):083101–083106. https://doi.org/10.1063/1.5037992.
6. Chakraborty S, Kumar H, Dasgupta C, Maiti PK.,(2017) Confined water: structure, dynamics, and thermodynamics. Acc. Chem. Res 50(9):2139–2146.https://doi.org/10.1021/acs.accounts.6b00617.
7. Giri AK, Teixeira F, NatáliaM, Cordeiro DS.,(2019) Salt separation from water using graphene oxide nanochannels: a

molecular dynamics simulation study. Desalination 460:1–14. https://doi.org/10.1016/j.desal.2019.02.014.

8. Giri AK, Teixeira F, Natália M, Cordeiro DS.,(2018) Structure and kinetics of water in highly confined conditions: a molecular dynamics simulation study. J. Mole. Liq. 268:625–636. https://doi.org/10.1016/j.molliq.2018.07.083.
9. Cheng C, Jiang G, Garvey CJ, Wang Y, Simon GP, Liu JZ, Li D.,(2016) Ion transport in complex layered graphene-based membranes with tuneable interlayer spacing. Sci. Adv. 2:1501272. https://doi.org/10.1126/sciadv.1501272.
10. Hong S, Constans C, Surmani Martins MV, Seow YC, Guevara Carrió JA, Garaj S .,(2017) Scalable graphene-based membranes for ionic sieving with ultrahigh charge selectivity. Nano Lett. 17:728–732. https://doi.org/10.1021/acs.nanolett.6b03837.
11. Alkurdi Susan S.A, Al-Juboori R.A, Bundschuha J, Hamawand I.,(2019), Bone char as a green sorbent for removing health-threatening fluoride from drinking water, J. Environment International.127,407-719. https://doi.org/10.1016/j.envint.2019.03.065.
12. Huang L, Zhang M, Li C, Shi G.,(2015), Graphene-Based Membranes for Molecular Separation, J. Physical Chemistry Letters.6.2806-2815. https:// doi.org/10.1021/acs.jpclett.5b00914.
13. Areiqat A, Mohamed K.A.,(2005), Optimization of the negative impact of power and desalination plants on the ecosystem,J.Desalination185.95-103. https://dio.org/10.1016/j.desal.2005.04.038
14. Guerrero J,Mahmoud A , Alam T , Sanchez A, Jones K.D, and Ernest A.,(2022), Collaborative Environmental Approach for Development of the Lower Laguna Madre Estuary Program Strategic Plan in South Texas, Journal of Environmental Informatics Letters, 7(1) , 1-1. https://doi:10.3808/jeil.202100075
15. Lattemann, S.; Hoepner, T.,(2008),Environmental impact and impact assessment of seawater desalination.Desalination,220, 1–15. https://doi.org/10.1016/j.desal.2007.03.009
16. Song, B., Zeng, G. M.; Gong, J. L., Liang, J., Xu, P.; Liu, Z. F., Zhang, Y., Zhang, C., Cheng, M.; Liu, Y. et al.,(2017) ,Evaluation methods for assessing effectiveness of in situ remediations of soil and sediment contaminated with organic pollutants and heavy metals. Environ. Int, 105, 43–55. https://doi.org/10.1016/j.envint.2017.05.001
17. Wang P, Zhan S, Xia Y, Ma S, Zhou Q, Li Y.,(2017) The fundamental role and mechanism of reduced graphene oxide in rGO/Pt-TiO_2 nanocomposite for high-performance photocatalytic water splitting Applied catalysis B: environmental the fundamental role and mechanism of reduced graphene oxide in rGO/Pt-TiO_2 nanocomposite for high-performance photocatalytic water splitting. (December). https://doi.org/10.1016/j.apcatb.2017.02.031
18. Parvizi-Majidi A, (2000) Whiskers and particulates. Comprehensive Composite Materials, pp 175–198. https://doi.org/10.1016/b0-08-042993-9/00045-0
19. Leong SK, Razmjou Chaharmahali A, Wang K, Hapgood K, Zhang X, Wang H.,(2014) TiO_2 based photocatalytic membranes: a review.J. Member. Sci. 472:167–184. https://doi.org/10.1016/j.memsci.2014.08.016
20. Zhang R-X, Braeken L, Luis P, Wang X-L, Van der Bruggen B.,(2013) Novel binding procedure of TiO2 nanoparticles to thin-film composite membranes via self-polymerized polydopamine. J.Membr Sci 437:179–188. https://doi.org/10.1016/j.memsci.2013.02.059
21. Xu C, Cui A, Xu Y, Fu X.,(2013) Graphene oxide–TiO_2 composite filtration membranes and their potential application for water purification.Carbon62:465–471. https://doi.org/10.1016/j.carbon.2013.06.035
22. Pi J-K, Yang H-C, Wan L-S, Wu J, Xu Z-K.,(2016) Polypropylene microfiltration membranes modified with TiO_2 nanoparticles for surface wettability and antifouling property. JMembr Sci 500:8–15. https://doi.org/10.1016/j.memsci.2015.11.014
23. Liu J, Van Der Bruggen B.,(2017) Author's accepted manuscript construction of TiO_2 @ graphene oxide incorporated antifouling nanofiltration membrane with elevated filtration performance. J Membr Sci. https://doi.org/10.1016/j.memsci.2017.03.040
24. Bhanvase, B. A., Shende, T. P., & Sonawane, S. H.,(2017). A review on graphene – TiO_2 and doped graphene –TiO_2 nanocomposite photocatalyst for water and wastewater treatment.2515(December 2016).https://doi.org/10.1080/21622515.2016.1264489
25. Ibrahim Q, Akbarzadeh R.,(2020).A photocatalytic TiO_2/graphene bilayer membrane design for water desalination: a molecular dynamics simulation. https://doi.org/10.1007/s00894-020-04422-4.
26. Sirk T. W., Moore S., Brown E. F.,(2013).Characteristics of Thermal Conductivity in Classical Water Models, J Chem Phys, 138, 064505, 123-137. https://doi.org/10.1063/1.4789961.
27. Plimpton S. J., Thompson A. P.(2012).Computational aspects of Many-Body potentials, MRS Bulletin, 37, 513-521. https://doi.org/10.1557/mrs.2012.96.
28. Fereidoon A, Aleaghaee S, Taraghi I.,(2015).Mechanical properties of hybrid graphene/TiO_2 (rutile) nanocomposite: a molecular dynamics simulation. Comput Mater Sci 102:220–227. https://doi.org/10.1016/j.commatsci.2015.02.044.
29. Lennard-Jones, J. E., "On the Determination of Molecular Fields", Proc. R. Soc. Lond. A, 106(738):463477,Bibcode:1924RSPSA.106..463J,https://doi.org/10.1098/rspa.1924.0082(1924).
30. Mayo Stephen L., Olafson Barry D., and Goddard William A. III,(1990), A Generic Force Field for Molecular Simulations, J. Phys. Chem. , 94, 8897-8909. https://doi.org/10.1021/j100389a010.
31. Soc J. Am. Chem.,(1992), for Molecular Mechanics and Molecular Dynamics Simulations. 114, 10024–10035. https://doi.org/10.1021/ja00051a040
32. Mayo S. L., Olafson B. D., & Goddard W. A., (1990). DREADING: a generic force field for molecular simulations. The Journal of Physical Chemistry, 94(26), 8897–8909. https://doi.org/10.1021/j100389a010.
33. Schrier J, (2010), Helium separation using porous graphene membranes, J. Phys. Chem. Lett. 1 (15) 2284-2287. https://doi.org/10.1021/jz100748x.
34. Wade A.D, Wang L.P, Huggins D.J,(2018), Assimilating Radial Distribution Functions to Build Water Models with Improved Structural Properties, http://pubs.acs.org on August 17, 2018.